International Journal of Computer Information Systems and Industrial Management Applications
ISSN 2150-7988 Volume 18 (2026) pp. 1-15

https://doi.org/10.70917/ijcisim-2026-3329
Article

# Intelligent Optimization of Spatial Parameters for Low-Carbon Campuses: A Study Based on Generative Design and Genetic Algorithms

**Yanqi Tang [1,*]**

[1] School of Art and Communication, Tianfu College of Southwestern University of Finance and Economics, Chengdu, Sichuan, 610051, China
* Correspondence author: 13880770171@163.com

**Abstract:** In order to improve the computability and multi-objective coordination ability of the spatial form design of low-carbon campuses, in this study, GIS data processing, parametric generative design and NSGA-II are used. Eight variables such as green space ratio, canopy cover, permeable paving ratio and road network density were hybrid-encoded, while the net life-cycle carbon emissions, outdoor thermal comfort, and walkability were set as the optimization objectives by taking a typical open space at Chengdu East Campus as a study case. The results indicate that 36 non-dominated solutions were obtained from the algorithm. The comprehensive balanced solution resulted in a reduction of the net carbon emissions from 148.6 $tCO_2e$ to 117.9 $tCO_2e$, an increase of the proportion of thermally comfortable area from 43.2% to 64.5% and an increase of walkability from 0.614 to 0.801. Spatial continuity, canopy supplementation and direct path connectivity allows for the synergic optimization of carbon reduction, environmental improvement and circulation efficiency within a limited site.

**Keywords:** low-carbon campus; spatial form; generative design; genetic algorithm; multi-objective optimization; life-cycle carbon emissions

## 1. Introduction

College campuses serve a variety of functions, including teaching, everyday life, and social interaction. Not only do they have an impact on land-use and activity patterns, but they also have a lasting impact on the use of materials, the use of energy in running and maintaining operations, carbon capture through vegetation, and the local thermal environment. Nowadays, however, carbon accounting in universities is progressively expanding to include energy, transport, materials, and operations; however, the majority of relevant findings are still at the level of emissions inventories and management, and there is no quantified representation of how the distribution of space, pavement, and vegetation structure influences carbon efficiency (Ahonen et al., 2024 [1]).

At the same time, parametric modeling can transform site boundaries, paths, green spaces, and facilities into continuous or discrete variables. But campus spaces are also affected by low carbon targets, thermal comfort, walking efficiency, and engineering constraints; a single goal or fixed weighting is difficult to accurately reflect the trade-offs between these performance metrics. Multiobjective evolutionary algorithms preserve feasible solutions for different performance preferences by nondominance ordering, which provides the technical basis for automatic searching for complex spatial solutions (Saadi, 2024 [2]; Fattahi Tabasi et al. 2024 [3]; Bilge and Yaman, 2025 [4]).

Furthermore, the environmental performance of campus open spaces is distinctly form-dependent. The canopy reduces the heat exposure by shading and transpiration, whereas the permeable pavement and the green space structure affect the surface heat transfer; the density of the road network and the layout of the nodes directly affect the walking distance and the efficiency of the use of space

(Jayasooriya et al., 2024 [5]; Ow and Chan, 2024 [6]). Therefore, low carbon campus spaces cannot be assessed solely on the basis of the ratio of green space or individual carbon emissions; rather, a performance framework that integrates carbon emissions, thermal comfort, and accessibility needs to be developed.

In view of the above problems, this paper integrates GIS site data, carbon emission factors, and parametric geometry models into the production design process, and uses eight morphological parameters, such as the ratio of green space, canopy cover, permeability paving ratio, and road network density, as chromosomes. NSGA-II defines net life cycle carbon emissions, outdoor thermal comfort, and walkability as parallel targets. By means of constraint checking, population iteration, and Pareto screening, the system can generate the campus space scheme with differentiated performance, thus making the transition from empirical to data-driven optimization.

## 2. Problem Description for Intelligent Optimization of Low-Carbon Campus Spatial Morphology

Optimization of low carbon campus space needs to change the design object from the graphic to the computable problem. This paper considers the site boundary, the preserved structure, the existing tree, the entry and exit, and the active node as the fixed input. A 1-meter spatial grid is used to uniformly map the site data to a metric coordinate system, and the geometric discreteness of a 1-meter space grid ensures that the different candidate schemes share the same computational scale (Caetano et al. 2024 [7]).

At the same time, however, changes in space have an impact on material input, carbon capture by plants, heat exposure, and cycle efficiency; thus, one target is not enough to fully describe low carbon performance. The document sets net life cycle carbon emissions as a minimum target, and the percentage of thermal comfort and walkability as maximum targets. That definition avoids that the systems that are created merely seek to increase the amount of green space to the detriment of spatial efficiency (Mavahebi Tabatabai et al., 2026 [8]).

Let the vector of spatial form parameters be:

$$\mathbf{x} = \left[x_1, x_2, \ldots, x_n\right]^{\mathrm{T}} \tag{1}$$

The multi-objective optimization problem is expressed as:

$$\begin{gathered}
\min_{x\in\Omega} \mathbf{F}\left(\mathbf{x}\right) = \left[\frac{C_{net}\left(\mathbf{x}\right)-C_{\min}}{C_{\max}-C_{\min}}, -\frac{R_{tc}\left(\mathbf{x}\right)-R_{\min}}{R_{\max}-R_{\min}}, -\frac{A_w\left(\mathbf{x}\right)-A_{\min}}{A_{\max}-A_{\min}}\right] \\
\Omega = \left\{\mathbf{x} \middle| l_i \le x_i \le u_i, g_j\left(\mathbf{x}\right) \le 0, q_k\left(\mathbf{x}\right) = 0\right\}
\end{gathered} \tag{2}$$

where $\mathbf{x}$ is the spatial morphology parameter vector; $n$ is the number of parameters; $C_{net}$ is the net carbon emissions over the life cycle; $R_{tc}$ is the proportion of thermally comfortable area; $A_w$ is walkability; $C_{\min}$, $C_{\max}$, $R_{\min}$, $R_{\max}$, $A_{\min}$, and $A_{\max}$ are the normalized bounds for each performance metric, respectively; $\Omega$ is the feasible solution space; $l_i$ and $u_i$ are the lower and upper bounds for the $i$ th morphology parameter; $g_j$ is the inequality constraint; and $q_k$ is the equality constraint.

The problem formulation combines spatial generation and performance calculation into a single data structure, which allows for geometric validity checks, carbon emissions accounting, and environmental performance assessments for each candidate solution. Lifecycle boundaries include materials, design, operation and maintenance, as well as carbon sequestration of plants, so that local reductions do not lead to a global carbon shift (Deda et al., 2025 [9]).

## 3. Spatial Optimization Method Based on Generative Design and Genetic Algorithms

### 3.1. Overall Technical Framework

The Spatial Form Optimization Framework is based on Site Data, Project Generation, Performance Feedback, and Decision Output, as illustrated in Figure 1, GIS Survey Data, Material Characteristics, Plant Configuration, Weather Conditions, and Space Use Records. These data, after the coordinate calibration, the spatial grid, the outlier removal, and the dimension standardization, form a standard data set that can be used by the parametric model. This process reduces the differences in size, format, and spatial precision between multiple sources, and provides a basis for precise mapping of morphological variables into site characteristics.

The Generation Layer converts green spaces, paths, pavements, trees, and shadows into adjustable geometric objects, and automatically generates candidate schemes based on the site boundaries, existing facilities, entry and exit distances, and minimum pass width. At the same time, the assessment layer calculates the net life cycle carbon emissions, outdoor thermal comfort and walkability, while returning the solution that exceeds the boundaries, overlaps, or has a path break in the generation layer for correction, thus avoiding disconnection between the spatial form and the environment performance (Abdollahzadeh and Biloria, 2024 [10]; Şimşek et al., 2025 [11]).

The decision layer uses the multiobjective population-based search to update the candidate schemes and screen for representative spatial forms. The data input, the geometry generation, the performance calculation, and the scheme update thus constitute a closed loop system, which allows the tracking of each parameter adjustment to the corresponding changes in the carbon performance, the heat environment, and the efficiency of use (Lisco and Szentes 2025 [12]).

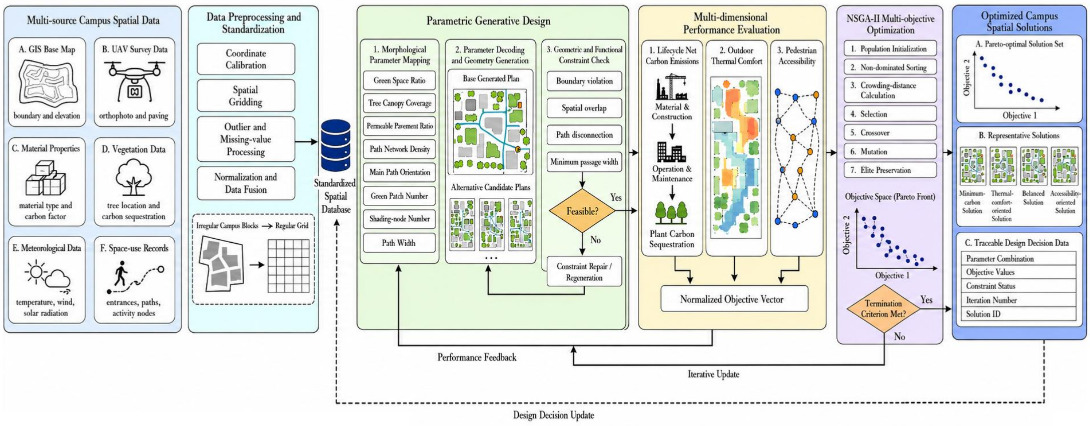


***Figure 1.*** Overall Technical Framework for Intelligent Optimization of Low-Carbon Campus Spatial Forms

## *3.2. Campus Spatial Data Acquisition and Preprocessing*

Data collection includes six types of information: site geometry, material, vegetation, weather, pedestrian traffic, and facility operations. Site boundaries, building contours, roads, and elevations are taken from the basic GIS map and unmanned aerial imagery; pavement type, tree position, canopy area, and material quantity are supplemented by field surveys and building records. Temperature, humidity, solar radiation, and walking paths are associated with the corresponding objects according to their spatial location. Carbon emissions calculations need to have uniform boundaries for activity data, emission factors, and spatial units to avoid duplication or omission when aggregating data from various sources (Garnevičius et al., 2025 [13]).

Multi-source data is first unified into a common coordinate system via affine transformation:

$$\tilde{\mathbf{p}}_i = \mathbf{A}\begin{bmatrix} e_i \\ n_i \\ 1 \end{bmatrix} \tag{3}$$

In the equation, $\tilde{\mathbf{p}}_i$ represents the transformed planar coordinates of the $i$ th object; $e_i$ and $n_i$ represent the original east and north coordinates, respectively; and $\mathbf{A}$ is the affine transformation matrix containing the translation, rotation, and scale correction parameters.

After coordinate unification, point based monitoring values are mapped to the spatial grid using a distance-weighted kernel function:

$$s_{ab}^{(m)} = \frac{\sum_{i=1}^{N_m} \omega_{iab}^{(m)} d_i^{(m)} \eta_i^{(m)}}{\sum_{i=1}^{N_m} \omega_{iab}^{(m)} \eta_i^{(m)} + \varepsilon}, \omega_{iab}^{(m)} = \exp\left[-\frac{\left\|\tilde{\mathbf{p}}_i - \mathbf{c}_{ab}\right\|_2^2}{2\rho_m^2}\right] \tag{4}$$

where $s_{ab}^{(m)}$ is the fused value for data class $m$ in the grid cell at row $a$ and column $b$; $N_m$ is the number of valid samples for this data class; $d_i^{(m)}$ is the $i$ th observation; $\eta_i^{(m)}$ is the data validity flag; $\omega_{iab}^{(m)}$ is the spatial distance weight; $\mathbf{c}_{ab}$ is the grid center coordinate; $\rho_m$ is the kernel bandwidth; and $\varepsilon$ is a small constant to prevent the denominator from becoming zero.

Data cleaning simultaneously checks for closed vector boundaries, path connectivity, object overlap, and missing attributes, and uses the interquartile range to suppress outliers:

$$r_{ab}^{(m)} = \operatorname{clip}\left(\frac{s_{ab}^{(m)} - \operatorname{Med}\left(S^{(m)}\right)}{\operatorname{IQR}\left(S^{(m)}\right) + \varepsilon}, -\kappa, \kappa\right) \tag{5}$$

where $r_{ab}^{(m)}$ is the robustly standardized result; $S^{(m)}$ is the set of grid data in class $m$; $\operatorname{Med}(\cdot)$ is the median; $\operatorname{IQR}(\cdot)$ is the interquartile range; $\kappa$ is the truncation threshold; and $\operatorname{clip}(\cdot)$ is used to limit the range of outliers.

The processed raster data, vector topology, and material properties are combined to form a unified spatial database. The uniform data structure preserves the boundaries of the site as well as the relationship between the facilities, and also provides reliable conversion of the green space ratio, the canopy cover, the permeable paving rate, and the road network density into numerical variables, thus reducing the scale differences in calculating and implementing the climate response strategy (Brandsma et al. 2024 [14]).

### *3.3. Encoding of Spatial Morphological Parameters*

However, genetic search still needs a uniform data carrier to organize chromosomes in accordance with the mapping relation "Space Object — Shape Attribute — Gene Location." Green Space Ratio, Canopy Cover, Permeable Paving, Road Density, Main Path, and Path Width are coded as Integer. This hybrid encoding preserves the granularity of continuous morphological adjustments while avoiding invalid decimals in facility counts following crossover and mutation.

Each gene is bound to a lower bound, an upper bound, a data type, and a spatial object identifier. The decoding program first returns the normalized genes to their true range, then rounds the discrete variables, and sends the results to the Geometric Generating Interfact. Parameter boundaries are defined together by the area of the site, the retained elements, the accessibility requirements, and the low carbon design conditions, so as to reduce the number of infeasible solutions in the search space. Multi-objective building optimization typically uses the design variables expressed as real-number genes with well-defined boundaries to maintain consistency between performance calculations and morphological adjustments (Alaili et al., 2025 [15]).

The parameter decoding process can be implemented using the following **Python functions**:

```python
from collections.abc import Mapping, Sequence
def decode_chromosome(
    chromosome: Sequence[float],
    bounds: Mapping[str, tuple[float, float]],
    discrete_genes: set[str],
) -> dict[str, float | int]:
    """Decode normalized genes into spatial morphology parameters."""
    if len(chromosome) != len(bounds):
        raise ValueError("Chromosome length does not match parameter bounds.")

    parameters: dict[str, float | int] = {}

    for gene, (name, limit) in zip(chromosome, bounds.items()):
```

```
        lower, upper = limit
        normalized_gene = min(max(float(gene), 0.0), 1.0)
        decoded_value = lower + normalized_gene * (upper - lower)

        parameters[name] = (
            int(round(decoded_value))
            if name in discrete_genes
            else decoded_value
        )

    return parameters
```

This coding structure makes sure that every chromosome has a unique set of space parameters, while preserving the name of the parameter, the number limit, and the variable type. The generating program can make use of the same data interface to reconstruct the path, map the green space, and the layout of the facility, while the function computing module can directly track the genetic source corresponding to the variation of each index.

## *3.4. Construction of Generative Spatial Schemes*

Chromosome decoding results are written into the parametric geometry engine. In this method, the site boundary, the preserved structure, the existing tree, the entrance and exit, and the fire path are considered as the fixed objects, and then the variable space is reconstructed according to the proportion of the green space, the density of the road, the main route, and the number of patches. Instead of random assembly, the program uses rules-based constraints; thus, each set of parameters can produce a unique, reproducible plan layout.

Green space units are assigned a comprehensive suitability score based on shading potential, thermal exposure, and path distance:

$$\psi_v = \alpha_1 \hat{H}_v + \alpha_2 \hat{T}_v - \alpha_3 \hat{D}_v - \alpha_4 \hat{O}_v \tag{6}$$

where $\psi_v$ is the green space configuration suitability for the $v$ th grid cell; $\hat{H}_v$ is the normalized shading potential; $\hat{T}_v$ is the normalized heat exposure intensity; $\hat{D}_v$ is the normalized distance from the grid cell to the main path; $\hat{O}_v$ is the degree of occupation by construction or retention elements; and $\alpha_1, \alpha_2, \alpha_3, \alpha_4$ are the respective weights.

In this algorithm, adjacent grid cells are selected according to their suitability, and the patches are formed by regional growth. The path system connects entrances, education spaces, and activity nodes, minimizing detour distances while complying with minimum width requirements. Priority should be given to trees and shade structures in areas where there is a high degree of heat exposure and high frequency of use, so as to ensure that the GI's cooling performance is in line with the demand for space activity (Sumaryana et al. 2024 [16]).

After generating candidate schemes, the program uses a composite constraint function to identify invalid layouts:

$$\Phi(G) = \lambda_1 A_{out} + \lambda_2 A_{overlap} + \lambda_3 N_{break} + \lambda_4 L_{deficit} \tag{7}$$

In the formula, $\Phi(G)$ represents the constraint violation value for the candidate geometric solution $G$; $A_{out}$ represents the out-of-bounds area; $A_{overlap}$ represents the object overlap area; $N_{break}$ represents the number of path breaks; $L_{deficit}$ represents the cumulative length that does not meet the minimum width requirement; and $\lambda_1, \lambda_2, \lambda_3, \lambda_4$ represents the penalty coefficient. When the constraint violation value is larger than zero, the program performs boundary clipping, object translation, path reconnection, and width correction; if the solution still does not satisfy the requirements, the program will immediately eliminate the solution.

## *3.5. Low-Carbon Spatial Performance Evaluation Model*

Once a viable space plan has been introduced into the performance computing module, the evaluation program retrieves the material utilization, the construction method, the maintenance frequency, the plant configuration, and the spatial grid properties according to a uniform object numbering system. Performance outputs include net life cycle carbon emissions, percentage of thermal comfort zone, and walkability. The CCS coverage includes the generation, construction, long term maintenance and carbon sequestration in power stations, thus avoiding the direct replacement of the actual emission reduction capacity by the proportion of green space (Paredes-Canencio et al., 2024 [17]).

$$C_{net} = \sum_{m=1}^{M} Q_m f_m + \sum_{\tau=1}^{Y} \frac{E_\tau f_e + W_\tau f_w + R_\tau f_r}{(1+\delta)^\tau} - \sum_{\tau=1}^{Y} \frac{\sum_{s=1}^{S} N_{s,\tau} q_{s,\tau}}{(1+\delta)^\tau} \tag{8}$$

where $C_{net}$ represents net life-cycle carbon emissions; $Q_m$ represents the quantity of material category $m$; $f_m$ is the corresponding material carbon emission factor; $M$ is the number of material categories; $E_\tau, W_\tau, R_\tau$ represent energy consumption, irrigation water use, and material replacement volume in year $\tau$, respectively; $f_e, f_w, f_r$ are the emission factors for energy, water use, and material replacement, respectively; $Y$ is the evaluation period; $\delta$ is the time discount rate; $N_{s,\tau}$ is the effective quantity of plant category $s$ in year $\tau$; $q_{s,\tau}$ is the annual carbon sequestration per plant; $S$ is the number of plant types.

Thermal environment assessment is performed at the grid cell level; the program calculates the thermal comfort index according to air temperature, humidity, wind velocity, average radiation temperature, and canopy shade. Local radiation and ventilation conditions are changed by building boundaries and canopy structures; thus, it is necessary to compare different morphological scenarios in the same weather season (Isinkaralar et al., 2025 [18]; Lindberg et al. 2025 [19]).

$$R_{tc} = \frac{\sum_{v=1}^{V} A_v \mathrm{I}(\theta_L \le P_v \le \theta_U)}{\sum_{v=1}^{V} A_v} \tag{9}$$

where $R_{tc}$ is the proportion of thermally comfortable area; $V$ is the number of spatial grid cells; $A_v$ is the area of the $v$ th grid cell; $P_v$ is the physiologically equivalent temperature of the corresponding grid cell; $\theta_L$ and $\theta_U$ are the lower and upper limits of the comfort range, respectively; and $\mathrm{I}(\cdot)$ is the conditional indicator function.

Walkability is calculated on the basis of the shortest distance between the entrance, the education node, the activity node, and the road network. The evaluation process also takes into account the path length and the network connectivity, thus preventing the algorithm from gaining a shallow low carbon advantage by reducing the number of paths and reducing the efficiency of the day on campus (Tavares et al., 2024 [20]).

$$A_w = \frac{\sum_{o=1}^{O}\sum_{d=1}^{D} \pi_{od} \exp - \mu L_{od}}{\sum_{o=1}^{O}\sum_{d=1}^{D} \pi_{od}} \cdot \frac{2E_g}{V_g (V_g - 1)} \tag{10}$$

where: $A_w$ represents walkability; $O$ denotes the number of entrances; $D$ denotes the number of destination nodes; $\pi_{od}$ represents the trip weight from entrance $o$ to node $d$; $L_{od}$ denotes the shortest distance in the road network; $\mu$ represents the distance decay coefficient; $E_g$ denotes the number of road network edges; $V_g$ denotes the number of road network nodes. Based on the solution ID, the three performance results are written into the target vector, so that the population iteration, the solution comparison, and the sensitivity analysis use the same data source.

## *3.6. Multi-objective Optimization Algorithm Based on NSGA-II*

The Performance Evaluation Module writes down the NPL, the percentage of thermal comfort, and walkability into each target vector. An initial set of 120 possible solutions is created and categorized according to the dominant relationship. As illustrated in Figure 2, the geometry generation, the constraint check, the performance calculation, and the population update are carried out in the same cycle; the individuals with out of bounds, overlapping, or path break problems are corrected prior to sorting, and those that cannot be corrected are eliminated from the population.

Individuals within the same non-dominant level maintain the dispersion of the solution set based on crowding distance:

$$D_i = \sum_{k=1}^{3} \frac{z_{i+1,k} - z_{i-1,k}}{z_k^{\max} - z_k^{\min} + \varepsilon} \tag{11}$$

where $D_i$ is the crowding distance of the $i$ th individual; $k$ represents the $k$ th term among the three optimization objectives; $z_{i+1,k}$ and $z_{i-1,k}$ are the objective values of adjacent individuals after sorting by the $k$ th objective, respectively; $z_k^{\max}$ and $z_k^{\min}$ are the maximum and minimum values, respectively, of the $k$ th objective in the current population; and $\varepsilon$ is a small constant to prevent the denominator from becoming zero. The crowding distance of boundary individuals is set to infinity to preserve solutions at both ends of the Pareto front.

The selection operation gives priority to the retention of an individual with a lower non-dominant rank and a greater crowding distance; the cross operation uses a simulated binary cross with a probability of 0.90, and a mutation probability of 0. 125 for each of the 8 morphogenes. After the parent and child groups have been combined, the procedure selects 120 individuals through elite retention, and the algorithm is terminated when the Hypervolume growth is below the threshold value for 200 or 20 successive generations. This type of multiobjective search maintains solution set coverage among design variables with significant performance conflicts (Benaddi et al., 2023 [21]).

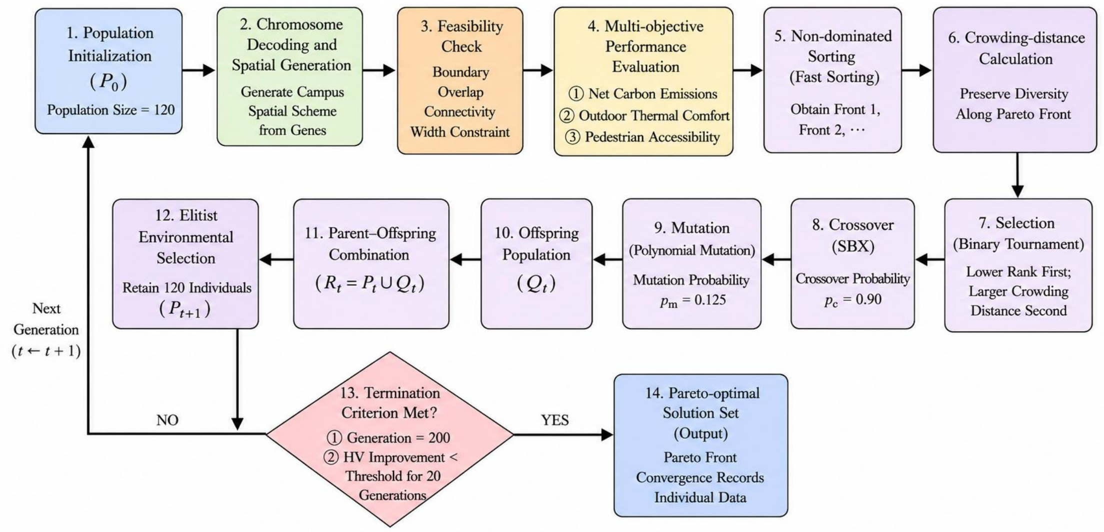


***Figure 2.*** NSGA-II-based multi-objective optimization workflow for spatial morphology

## *3.7. Method for Screening Integrated Optimization Solutions*

The non-dominated solutions produced by the NSGA-II exhibit different benefits in terms of carbon emissions, thermal comfort, and walkability; the simple optimization of one target can easily result in an imbalance in spatial functionality. First, the selection process keeps the three boundary solutions — those with the lowest CO2 emissions, the highest thermal comfort, and the most walkability — and then the rest of the solutions are ranked in an overall order. Then, the three targets are transformed into loss directions and normalized according to the extreme value of the current Pareto solution set.

The score for a comprehensive solution is defined as:

$$S_i = \sqrt{\sum_{k=1}^{3} w_k \left( \frac{f_{ik} - f_k^*}{f_k^{nad} - f_k^* + \varepsilon} \right)^2} + \beta\sigma_i - \gamma\xi_i \tag{12}$$

where $S_i$ is the comprehensive score of the $i$ th candidate solution; $f_{ik}$ is the loss value of the $i$ th solution for the $k$ th objective; $f_k^*$ is the ideal value for the $k$ th objective; $f_k^{nad}$ is the corresponding worst-case reference value; $w_k$ is the objective weight, defaulting to 1/3; $\sigma_i$ is the performance fluctuation coefficient of the morphological parameters under ±5% perturbation; $\xi_i$ is the normalized margin for boundary, width, and connectivity constraints; $\beta$ and $\gamma$ are the robustness penalty coefficient and feasibility reward coefficient, respectively; $\varepsilon$ is a small constant.

The selection process ranks candidate solutions in ascending order of composite scores, giving priority to those with a shorter target distance, less perturbation fluctuations, and greater constraint margins. At the same time, designers review parameter combinations, spatial layout, and three types of performance measures to avoid a situation in which the numerical optimal solution leads to fragmented green spaces, circuitous routes, or crowded facilities. The final output consists of three border scenarios and one integrated balanced scenario, which provides a consistent reference for morphological comparison, performance verification, and parameter interpretation of typical campus spaces.

## 4. Case Studies and Experimental Design for Typical Campus Spaces

### *4.1. Site Overview and Existing Low-Carbon Challenges*

The case study was chosen to be an open space located in the intersection between the academic and residential areas in Chengdu East Campus. It is a place for inter-class movement, short-term sojourn and daily socializing. The five objects types, namely building boundaries, existing trees, paving, entrances and exits, and activity nodes, were unified in the same coordinate system in a unified spatial database. On-site surveys were done to confirm material types, continuity of paths and canopy cover.

Current limitations are mostly a too high percentage of hard surfaces, disjointed green areas, and lack of continuous canopy coverage of trees and detours in the main paths, as seen in Table 1. The spatial deficits have also been shown to have a negative impact on the carbon footprint of materials, the exposure to heat in summer, and the overall pedestrian network connections. Hence, this case study is able to test the effectiveness of the three objectives evaluation, geometric generation and constraint remediation.

***Table 1.*** Basic Parameters of the Case Study Site and Existing Low-Carbon Issues

| Parameter Category | Basic Parameters | Data Acquisition Method | Existing Characteristics | Low-Carbon Issues | Optimization Mapping |
|---|---|---|---|---|---|
| Site Boundaries | Total Site Area, Renovable Area | GIS Surveying and On-Site Verification | Clear building and fire safety boundary restrictions | Limited scope for spatial adjustments | Geometrically Generated Boundaries |
| Paving System | Ratio of hard paving to permeable paving | Orthophoto Classification and Material Survey | Large areas of continuous hard paving | Materials have high embodied carbon and high surface heat storage | Percentage of Permeable Paving |
| Green Space System | Green Space Ratio, Number of Patches, Average Patch Area | GIS zoning statistics | Fragmented green space distribution | Insufficient carbon sink continuity and ecological connectivity | Green Space Ratio and Number of Patches |
| Tree System | Number of Trees, Canopy Cover | Drone imagery and field surveys | Uneven distribution of tree canopies in primary activity areas | Lack of consistent shade in areas with high heat exposure | Canopy Cover |
| Pathway system | Road network density, connectivity, and detour coefficient | Road network topology calculations | Indirect connections between some nodes | Increased walking distance and reduced spatial efficiency | Road Network Density and Path Direction |
| Service Facilities | Number of shaded nodes and rest areas | On-site inventory and coordinate recording | Mismatch between node configuration and pedestrian traffic hotspots | Insufficient thermal comfort in resting areas | Number of Shade Points |
| Thermal Environment | Proportion of areas with thermal exposure vs. proportion of comfortable areas | Microclimate grid simulation | Higher thermal loads in areas with concentrated paving | Restrictions on outdoor activities in summer | Thermal comfort target values |

### *4.2. Spatial Morphological Variables, Evaluation Parameters, and Experimental Setup*

The experimental design modified the spatial variables but the existing buildings, fire lanes, existing trees and main entrances/exits were retained. Table 2 indicates that the eight morphological variables were coded as a mix of continuous and integer variables. Of these, green space ratio, canopy cover, permeable paving ratio and road network density control the general spatial structure, path orientation, number of patches, shaded nodes and walkway width control the local spatial layout. Parameter boundaries were set to prevent spatial distortion from extreme values, due to area limits for renovation, and accessibility.

The grid size used for calculating the performance was always 1m × 1m, and the life cycle boundary was 30 years while typical summer heatwave periods were used. 120 individuals, 200 iterations of generations, crossover rate of 0.90, and mutation rate of 0.125 were used for the algorithm which was independently repeated 10 times. The uniform settings make sure that the effect of random initializations on the distribution of the non-dominating solutions is minimized and that different scenarios can be compared at the same data scale.

***Table 2.*** Spatial Morphological Variables, Evaluation Parameters, and Algorithm Experimental Settings

| Parameter Category | Variable or Parameter | Value Range or Setting | Data Type/Unit | Purpose of Setting |
|---|---|---|---|---|
| Spatial Form Variables | Green Space Ratio | 30%–55% | Continuous variable/% | Controls total green space area and carbon sink space |
| | Tree Canopy Cover | 20%–45% | Continuous variable/% | Regulating Shade Coverage and Heat Exposure Levels |
| | Permeable Paving Ratio | 25%–60% | Continuous variable/% | Adjusting material structure and heat exchange with the ground surface |
| | Road network density | 0.80–1.60 | Continuous variable/(km·ha$^{-1}$) | Control of Path Coverage and Connectivity Efficiency |
| | Main Path Direction | 0–180 | Continuous variable/(°) | Adjusting the Connection Direction Between Entrances and Activity Nodes |
| | Number of Green Spots | 3–8 | Integer variable/units | Controls green space concentration and spatial continuity |
| | Number of Shade Nodes | 4–12 | Integer variable/units | Adjusting Shade Configuration in High-Frequency Activity Areas |
| | Main Path Width | 2.0–4.5 | Continuous variable/m | Balance between traffic capacity and space utilization |
| Evaluation Parameters | Spatial calculation grid | 1×1 | m | Unified Scale for Carbon Emissions and Thermal Environment Calculations |
| | Life Cycle Assessment Period | 30 | years | Calculate materials, operation and maintenance, and plant carbon sequestration effects |
| | Thermal Environment Calculation Period | 12:00–16:00 | Typical summer day | Capturing Spatial Variations in Periods of High Heat Exposure |
| | Accessibility Analysis Objects | Entrance—Activity Node | Shortest Paths in the Road Network | Evaluating Travel Distance and Network Connectivity |
| | Number of Targets | 3 | | Corresponding to net carbon emissions, thermal comfort, and accessibility |

## *4.3. Analysis of the Genetic Algorithm Convergence Process*

120 spatial schemes have been used as initial population. The percentage of feasible solutions in the first generation was 71.7%, in 40th generation it was 91.7% and in 100th generation the percentage of feasible solutions was 97.5% after constraint refinement. It can be seen in Figure 3 that the hyper-volume rose from 0.412 to 0.771, with 68.5% of the increase occurring during the first 60 generations; The optimal net lifecycle carbon emissions value dropped from 148.6 $tCO_2e$ to 113.2 $tCO_2e$; The percentage of thermally comfortable area increased from 43.2% to 67.9% and walkability rose from 0.614 to 0.824.

The percentage increase per generation for all three objectives was below 0.3% after the 156th generation and the increase in Hypervolume was always less than 10 −4from the 178th generation to the 197th generation. The mean, standard deviation and coefficient of variation of the final Hypervolume from 10 independent runs were 0.768, 0.009, and 1.17%, respectively. As a result, hybrid encoding, geometric repair and elite retention were able to minimize the number of invalid individuals and to ensure that the population can gradually move towards the non-dominant frontier while retaining the spread of the solution set.

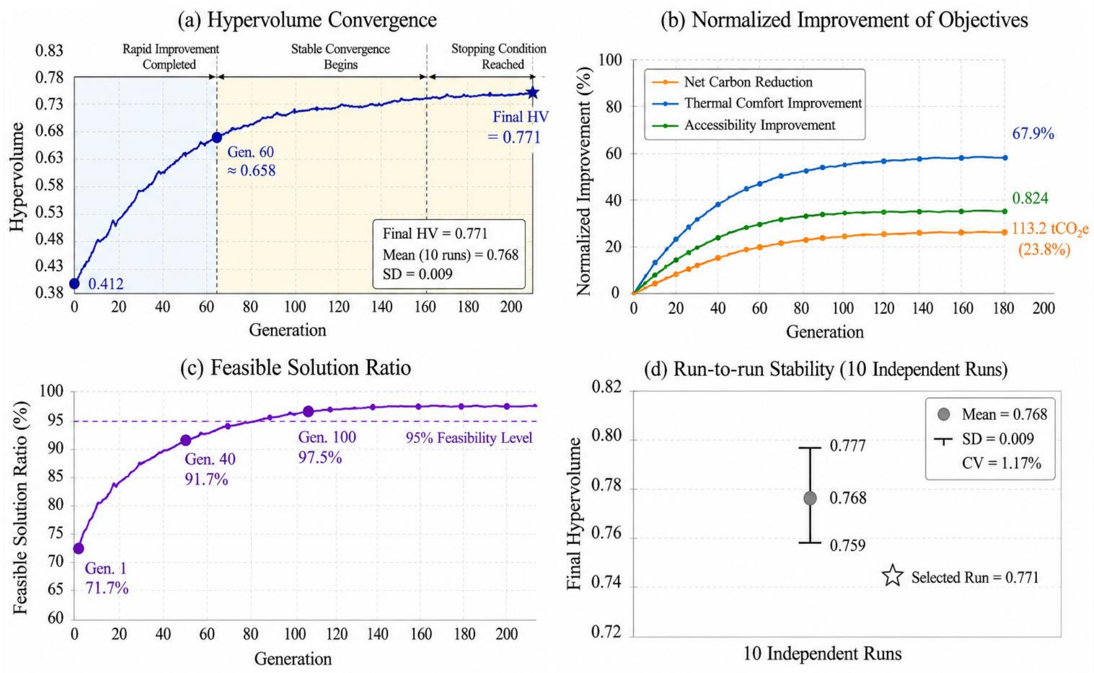


***Figure 3.*** Convergence process of NSGA-II multi-objective optimization

## *4.4. Pareto Front and Multi-Objective Trade-offs*

Once the population stabilises, 36 non-dominant solutions are created. As presented in Figure 4, the net lifetime carbon emissions vary between 113.2 and 126.4 tons of $CO_2$ equivalent, the percentage of the thermal comfort zone between 58.6% and 67.9% and the walkability between 0.742 and 0.824. The elite retention and congestion distance mechanisms did not cause the solutions to cluster in a small performance area in the 3D objective space, as the solution set was continuously distributed.

The low-carbon scenario has 113.2 tons of $CO_2$ equivalent, 58.6% and 0.742; the thermal comfort priority scenario has 126.4 tons of $CO_2$ equivalent, 67.9% and 0.768; the accessibility priority scenario has 122.8 tons of $CO_2$ equivalent, 60.7% and 0.824. The comprehensive balance scenario results in 117.9 tons of $CO_2$ equivalent, 64.5% and 0.801. It has 4.7 tons of $CO_2$ equivalent higher carbon emissions than the lowest value, but has improved its thermal comfort by 5.9 percentage points and accessibility by 0.059. The results indicate that the enlargement of the green space and canopy of the trees may be advantageous for thermal environment, while if the sidewalks become too full of trees, the efficiency of the traffic may decrease. This makes it quite apparent that there is a potentially important nonlinear trade-off between these three goals.

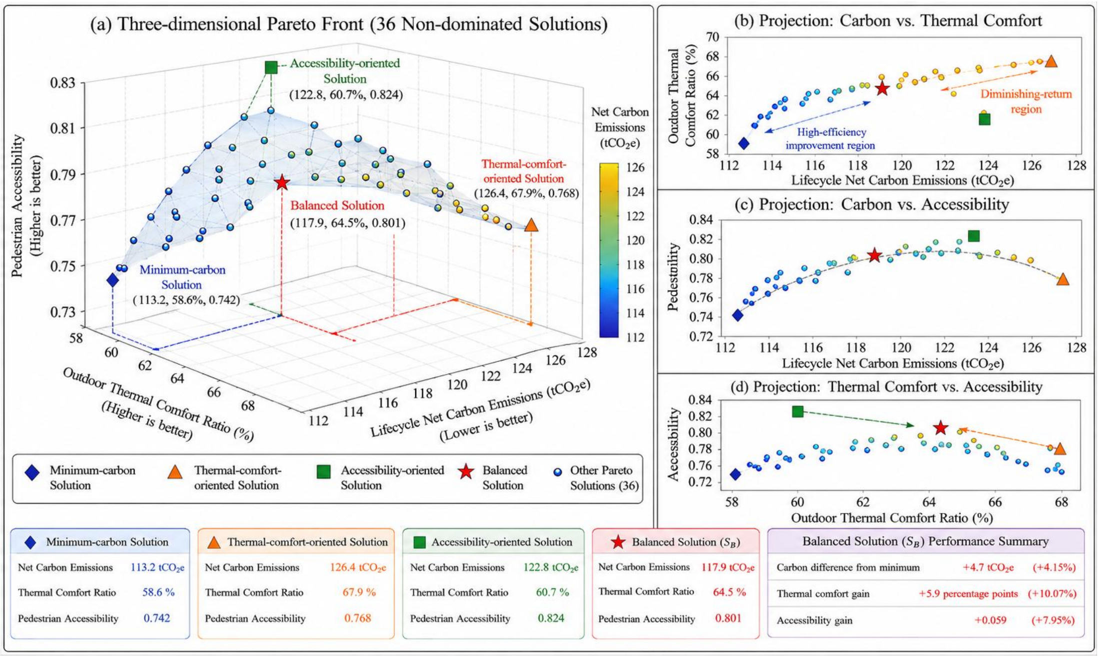


***Figure 4.*** Pareto front for life-cycle carbon emissions, thermal comfort, and walkability

## *4.5. Comparison of Low-Carbon Performance Before and After Optimization*

The comprehensive balanced solution (with the existing space as unity baseline) was identified as the scenario corresponding to 117.9 $tCO_2e$, 64.5%, and 0.801 through Pareto screening. As presented in Table 3, carbon emissions from materials and construction were reduced by 19.8 $tCO_2e$, carbon emissions from operation and maintenance for 30 years were reduced by 3.9 $tCO_2e$ and carbon sequestration by vegetation increased by 7.0 $tCO_2e$. This resulted in a net reduction in lifecycle carbon emissions from 148.6 $tCO_2e$ to 117.9 $tCO_2e$ (a 20.7% reduction).

Spatial restructuring has led to an improvement in both environmental and accessibility performance. The percentage of thermally comfortable areas rose by 21.3%, the average shortest walking distance was decreased by 34.4 m, and walkability increased by 30.5%. The results show that the continuous green spaces, canopy supplementation, replacement with permeable paving and the direct path connection can have synergistic effects and not just a response with increased green cover to improve performance.

***Table 3.*** Comparison of Performance Between the Existing Scheme and the Comprehensive Optimization Scheme

| **Performance Category** | **Evaluation Indicators** | **Existing Plan** | **Comprehensive Optimization Scheme** | **Absolute Change** | **Relative Change** |
|---|---|---|---|---|---|
| Construction Carbon Emissions | Carbon Emissions from Materials and Construction / $tCO_2e$ | 132.4 | 112.6 | −19.8 | −15.0% |
| Carbon Emissions from Operations and Maintenance | 30-Year Operations and Maintenance Carbon Emissions / $tCO_2e$ | 38.7 | 34.8 | −3.9 | −10.1% |
| Plant Carbon Sink | 30-Year Plant Carbon Sequestration / $tCO_2e$ | 22.5 | 29.5 | +7.0 | +31.1% |
| Overall Carbon Performance | Net Life Cycle Carbon Emissions/$tCO_2e$ | 148.6 | 117.9 | −30.7 | −20.7% |
| Thermal Environmental Performance | Proportion of Thermally Comfortable Area /% | 43.2 | 64.5 | +21.3 percentage points | +49.3% |
| Walking Efficiency | Average shortest walking distance / m | 146.8 | 112.4 | −34.4 | −23.4% |
| Road Network Performance | Walkability | 0.614 | 0.801 | +0.187 | +30.5% |

## *4.6. Analysis of Spatial Characteristics of Typical Optimization Schemes*

See Figure 5, in the existing space the green space ratio is 31.8%, canopy cover is 21.6% and permeable paving ratio is 27.4% and there are eight small green areas which are scattered in between making it difficult to create continuity of shade as shown in figure 5. The Lowest-Carbon Scenario keeps the percentage of green space at 44.1%, but makes the patches into four and decreases the material carbon footprint by using 54.6% permeable paving ratio, although the density of road networks is 0.92 km/ha, which limits the improvement of accessibility.

For the Thermal Comfort Priority scenario, canopy cover was increased to 44.2%, and 12 shading nodes were added, while for the Accessibility Priority scenario, road network density and walkway width were increased to 1.54km/ha and 4.3m, respectively. The comprehensive balanced scheme is designed based on a green space ratio of 46.8%, a canopy cover of 37.6%, a ratio of permeable paving of 51.2% and a road network density of 1.26 km/ha, which creates harmony between continuous green spaces, shaded nodes and direct pathways.


***Figure 5.*** Comparison of Spatial Morphology Between the Existing Scheme and a Typical Pareto-Optimized Scheme

## *4.7. Sensitivity Analysis of Spatial Morphology Parameters*

The sensitivity analysis focused on the comprehensive balanced scheme with 5% local perturbations in continuous variables and 1-level perturbations of green space patches and shaded nodes and noting the normalized changes in the three performance variables. The three parameters, green space ratio, canopy cover and road network density are the main sources of spatial performance variation, as shown in Table 4.

A higher green space ratio can have a direct effect of abating the net carbon emission and enhancing the thermal comfort at the same time and decrease some circulation space, sensitivity coefficient of canopy cover to thermal comfort is 0.92, and to accessibility is −0.16. The sensitivity coefficient of the density of road network to accessibility is 0.95 while the carbon emissions from paved surfaces are also increased. The main focus points for the permeable pavement ratio are for carbon performance, as are the path orientations and shaded nodes, for local adjustments.

***Table 4.*** Sensitivity and Importance Ranking of Spatial Morphological Parameters

| Spatial Morphology Parameters | Sensitivity Coefficient for Net Carbon Emissions | Sensitivity Coefficient for Thermal Comfort | Sensitivity Coefficient for Walkability | Composite Importance | Ranking |
|---|---|---|---|---|---|
| Green Space Ratio | −0.84 | 0.78 | −0.31 | 0.643 | 1 |
| Tree canopy cover | −0.61 | 0.92 | −0.16 | 0.563 | 2 |
| Road network density | 0.43 | −0.25 | 0.95 | 0.543 | 3 |
| Permeable Paving Ratio | −0.81 | 0.39 | 0.07 | 0.423 | 4 |
| Main Trail Width | 0.38 | −0.14 | 0.66 | 0.393 | 5 |
| Number of green patches | 0.33 | −0.46 | −0.22 | 0.337 | 6 |
| Number of shading nodes | 0.19 | 0.71 | 0.10 | 0.333 | 7 |
| Main path direction | 0.06 | 0.29 | 0.45 | 0.267 | 8 |

Note: Positive values indicate that an increase in the parameter leads to an increase in the corresponding evaluation metric, while negative values indicate that an increase in the parameter leads to a decrease in the corresponding evaluation metric; a decrease in net carbon emissions indicates improved low-carbon performance.

## 4.8. Comparison of Performance Among Different Optimization Methods

Each method employed the same data for the site and eight morphological variables and used 24, 000 solution evaluations. The Hypervolume of the random search method was only 0.602 with the reduction of net carbon emission to 116.8 $tCO_2e$, however thermal comfort and accessibility were 56.4% and 0.736 respectively, as shown in Table 5; this means that using a single-objective genetic algorithm, one criterion tends to be compromised for the optimization of another.

Weights in genetic algorithm were fixed and the weighted genetic algorithm obtained a Hypervolume of 0.711, which was subjected to restricted coverage of the feasible solution set. NSGA-II attained a Hypervolume of 0.768 and a ratio of feasible solution of 97.5%, while the integrated solution, in turn, attained a Hypervolume of 0.801 and a ratio of feasible solution of 64.5% and a feasible solution ratio of 117.9 $tCO_2e$. The runtime was found to grow by 6.3% from the weighted genetic algorithm but the number of nondominated solutions was 36, which gave more comprehensive performance trade-off space.

***Table 5.*** Comparison of Performance Among Optimization Methods for Different Spatial Forms

| **Optimization Method** | **Net Lifecycle Carbon Emissions/ $tCO_2e$** | **Proportion of Thermally Comfortable Area / %** | **Walkability** | **Hypervolume** | **Proportion of Feasible Solutions / %** | **Number of non-dominant solutions/number** | **Runtime / h** |
|---|---|---|---|---|---|---|---|
| Rule-of-thumb design | 134.7 | 52.8 | 0.692 | 0.487 | 100.0 | 1 | 1.8 |
| Random search | 125.9 | 57.6 | 0.748 | 0.602 | 76.3 | 11 | 2.6 |
| Single-objective genetic algorithm | 116.8 | 56.4 | 0.736 | 0.648 | 88.9 | 8 | 2.9 |
| Weighted Genetic Algorithm | 121.3 | 61.8 | 0.783 | 0.711 | 94.2 | 19 | 3.2 |
| NSGA-II | 117.9 | 64.5 | 0.801 | 0.768 | 97.5 | 36 | 3.4 |

# 5. Conclusion

The parametric coding, performance calculation, and multi-objective search of generative design and NSGA-II are employed to turn the spatial form adjustment of campus from an empirical process to an optimization process. This comprehensive balanced solution leads to an improvement in the net lifecycle carbon emissions (from 148.6 $tCO_2e$ to 117.9 $tCO_2e$), the proportion of thermally comfortable areas (from 43.2% to 64.5%) and the walkability (from 0.614 to 0.801). Results suggest that there is a synergy between continuity of green spaces, canopy supplementation, replacement of impervious paving and direct path connectivity. They also validate the literature on existing studies of generative design and its ability to provide performance trade-offs, as well as the effect of spatial form on the thermal environment. These conclusions, however, are limited to a single campus site, typical meteorological periods and regional carbon factors. Future studies can include multi-campus samples, real time environmental monitoring and agent based models to verify the resiliency of the boundaries of the parameters and pareto solutions for different climatic conditions and usages.

**Funding**

This work was supported by: Tianfu College of Southwestern University of Finance and Economics, under the 2026 major special project for university-level discipline cultivation. The project is titled: Research on Low-Carbon Transformation Paths and Management Mechanisms for Campus Environmental Spaces under Carbon Peaking and Carbon Neutrality Goals.The project number is: XCTF2026ZD12.

**References**

1. Ahonen V L, Woszczek A, Baumeister S, et al. Carbon neutral higher education institutions: a reality check, challenges and solutions[J]. International Journal of Sustainability in Higher Education, 2024, 25(9): 293-315.
2. Saadi J I, Chong L, Yang M C. The effect of targeting both quantitative and qualitative objectives in generative design tools on the design outcomes[J]. Research in Engineering Design, 2024, 35(4): 409-425.

3. Fattahi Tabasi S, Rafizadeh H R, Andaji Garmaroudi A, et al. Optimizing urban layouts through computational generative design: density distribution and shape optimization[J]. Architectural Engineering and Design Management, 2024, 20(5): 1164-1184.
4. Bilge E Ç, Yaman H. Multi-objective early-stage design optimization of multifamily residential projects[J]. International Journal of Architectural Computing, 2025, 23(2): 446-463.
5. Jayasooriya V M, Sirimanne A P, Silva R M, et al. Role of Urban Trees in Enhancing the Thermal Comfort of Rapidly Urbanizing Cities: An Analysis of Tropical Asian Tree Species Based on Physiological Equivalent Temperature (PET)[J]. Arboriculture & Urban Forestry, 2024, 50(5): 326-345.
6. Ow L F G, Chan E. Enhancing outdoor comfort in urban hot climates: investigating the cooling impact of two tropical trees through shade provision and transpiration[J]. Arboricultural Journal, 2024, 46(4): 272-291.
7. Caetano I, Pereira I, Leitão A. Balancing design intent and performance: an algorithmic design approach[J]. Architectural Science Review, 2024, 67(3): 255-267.
8. Mavahebi Tabatabai G, Tahsildoost M, Ardekani A, et al. Optimizing urban block layouts and density distribution: a generative design framework for neighborhood performance[J]. Smart and Sustainable Built Environment, 2026, 15(5): 1722-1750.
9. Deda D, Gervasio H, Quina M J. Advancing carbon footprint in higher education: an integrated assessment model[J]. The International Journal of Life Cycle Assessment, 2025, 30(9): 1930-1943.
10. Abdollahzadeh N, Biloria N. Solar performance-driven urban development: the case of western Sydney, Australia[J]. Advances in Building Energy Research, 2024, 18(5): 475-494.
11. Şimşek U Y, Kuş B, Özgen B. Evolutionary Algorithms: Creative Applications in the Early Design Phase[J]. Technology| Architecture+ Design, 2025, 9(1): 98-115.
12. Lisco M, Szentes H. Exploring the combined impact of generative design and reuse-centred design[J]. Engineering, Construction and Architectural Management, 2025, 32(13): 501-517.
13. Garnevičius M, Ševičienė V, Grubliauskas R, et al. Sustainability and carbon footprint evaluation at university: case study of VILNIUS TECH[J]. Technological and Economic Development of Economy, 2025, 31(6): 2105-2130.
14. Brandsma S, Lenzholzer S, Carsjens G J, et al. Implementation of urban climate-responsive design strategies: an international overview[J]. Journal of Urban Design, 2024, 29(5): 598-623.
15. Alaili, K., Tedjditi, A.K., Moutaouakil, E.M. et al. Optimizing building envelope design across various French climates: A multi-objective approach using NSGA II and RMP method. Build. Simul. 18, 1677–1696 (2025). https://doi.org/10.1007/s12273-025-1280-4.
16. Sumaryana H, Buchori I, Sejati A W. Green infrastructure modelling for UHI control to urban thermal comfort: a case study of Temanggung urban area[J]. International Journal of Urban Sciences, 2024, 28(2): 211-243.
17. Paredes-Canencio K N, Lasso A, Castrillon R, et al. Carbon footprint of higher education institutions[J]. Environment, Development and Sustainability, 2024, 26(12): 30239-30272.
18. Isinkaralar O, Isinkaralar K, Sevik H, et al. Thermal comfort modeling, aspects of land use in urban planning and spatial exposition under future climate parameters[J]. International Journal of Environmental Science and Technology, 2025, 22(12): 11977-11990.
19. Lindberg F, Wallenberg N, Thorsson S, et al. Micro-scale, city-wide analysis of outdoor thermal comfort during heatwaves in high latitude cities: influence of building geometry and vegetation[J]. International Journal of Biometeorology, 2025, 69(12): 3421-3434.
20. Tavares S G, Wesener A, Fox-Kämper R, et al. Urban comfort and adaptive capacity: an exploratory study of urban life and climate responses in Aachen, Germany[J]. Cities & Health, 2024, 8(4): 666-683.

21. Benaddi F Z, Boukhattem L, Ait Nouh F, et al. Energy-saving potential assessment of a classroom building envelope through sensitivity analysis and multi-objective optimization under different climate types[J]. Building Services Engineering Research & Technology, 2023, 44(3): 309-332.

**About the Author**

**Yanqi Tang** was born in 1993 in Chengdu, Sichuan Province, People's Republic of China. She graduated from Sichuan Agricultural University with a master's degree and currently serves as a lecturer at Tianfu College of Southwestern University of Finance and Economics, where she also holds the title of Landscape Architecture Engineer. Her research interests include low-carbon landscapes, ecological landscapes, rural landscapes, and urban renewal.